ISSN 1392–1320 MATERIALS SCIENCE (MEDŽIAGOTYRA). Vol. 21, No. 2. 2015

Structural and Electronic Properties of CuO, CuO_2 and Cu_2O Nanoclusters – a DFT Approach

Sriram SUBRAMANIAN, Rubalya VALANTINA, Chandiramouli RAMANATHAN *

Department of Physics, School of Electrical & Electronics Engineering, SASTRA University, Tirumalaisamudram, Thanjavur-613401, Tamilnadu, India

crossref http://dx.doi.org/10.5755/j01.mm.21.2.6459

Received 14 February 2014; accepted 11 September 2014

The realistic structures of CuO, CuO_2 and Cu_2O were completely optimized using density functional theory approach. The different structures were optimized to study the structural stability, dipole moment, point symmetry, HOMO-LUMO gap, ionization potential, electron affinity and binding energy of CuO, CuO_2 and Cu_2O. The electronic properties of clusters were discussed in terms of HOMO-LUMO gap, density of states, ionization potential and electron affinity. This information will provide an insight for the synthesis of nanomaterials with proper geometry which finds its potential importance in engineering applications.

Keywords: ionization potential**,** electron affinity, nanoclusters, HOMO-LUMO, binding energy.

1. INTRODUCTION

Oxygen combines with copper to form copper (I) oxide (Cu_2O), copper (II) oxide (CuO) and copper dioxide (CuO_2). These oxides of copper can bond with one or two electrons. Oxygen may form compound with metals by gaining two electrons, which may accept one electron from each of two copper atoms forming copper (I) oxide or it may accept two electrons from one atom, which forms copper (II) oxide. Cu_2O is a p-type semiconductor also called as cuprous oxide; the potential application of Cu_2O is in agriculture, used as an ingredient in many fungicides that protect from fungal diseases. It is also active component in antifouling paints [1], pigment in some types of glass [2], in ceramic glazes [3], as catalyst in chemical processes, photovoltaic and photocatalytic applications [4 – 7]. CuO is also known as cupric oxide; CuO is added to clay glazes as pigment [8] and used as abrasive for polishing lenses and optical components [9]. CuO_2 is one of the important compounds in superconducting lattice [10 – 12]. The preparation of CuO, CuO_2 and Cu_2O in thin film form or as nanoparticles involves various methods such as thermal evaporation, RF sputtering, laser ablation, chemical vapour deposition, chemical bath deposition, sol-gel method, spray pyrolysis and electrodeposition methods [13 – 16]. The morphology such as nano needles, nanoflakes, nano rods and nanotube can be synthesized by proper controlling mechanism [17 – 19]. The nanoclusters can be formed by proper synthesis of the material in the plane oriented substrates or by capping the material through surfactant. The motivation of the present work is since CuO, CuO_2 and Cu_2O find its potential application; if the morphology and structure is properly tailored it will be suitable for engineering applications.

With this as motivation, survey was conducted in Scirus database and it was found that much work has not been carried out in tailoring the morphology of copper oxides. The density functional theory (DFT) approach is one method to study the structural and electronic properties which can be used to synthesis a new form of materials depending on their engineering applications. In this article an attempt has been made to study the properties of the realistic structures of CuO, CuO_2 and Cu_2O nanoclusters.

2. COMPUTATIONAL METHODS

The possible structures of CuO, CuO_2 and Cu_2O clusters were completely optimized using NWChem package [20]. NWChem package is used to simulate complex biological and chemical structures for calculating in large scale. The conventional methods utilize Hartree-Fock calculation, which is carried out with a local basis set named as Fock build. In NWChem an algorithm known as Kohn-Sham matrix element is used to do the computation and energy convergence in DFT calculation. The electron correlation in DFT is taken into consideration through the exchange energy that arises from the antisymmetry of quantum mechanical wave function and dynamic correlation is used for the motion of the discrete electrons. DFT method involves the pseudo potential approximation to replace the complex effects of the bound electrons in the atom of the cluster that modifies the potential term of Schrödinger equation. The DFT method is exploited by using hybrid B3LYP exchange correlation for CuO, CuO_2 and Cu_2O clusters with 6-31G basis set [21 – 24]. The atomic number of copper and oxygen are 29 and 8 respectively, 6-31G is a proper basis set to optimize the nanoclusters. In the present study, B3LYP/6-31G basis set is used throughout for all the structures. The energy convergence in the order of 10^{-5} eV is achieved in the present work.

* Corresponding author. Tel.: +919489566466; fax.: +914362264120. E-mail address: *rcmoulii@gmail.com* (Ch. Ramanathan)

3. RESULTS AND DISCUSSION

3.1. Structures of CuO, CuO_2 and Cu_2O clusters

Fig. 1 shows the various structures of CuO, CuO_2 and Cu_2O clusters. In the structure of CuO-1, the Cu atom and O atoms have hexagonal pattern like structure with Cu and O atoms attached alternatively, CuO_2-1 structure has two Cu atoms and four O atoms in the form of hexagonal structure, in Cu_2O-1 structure it has two O atoms attached to four Cu atoms forming a hexagonal structure.

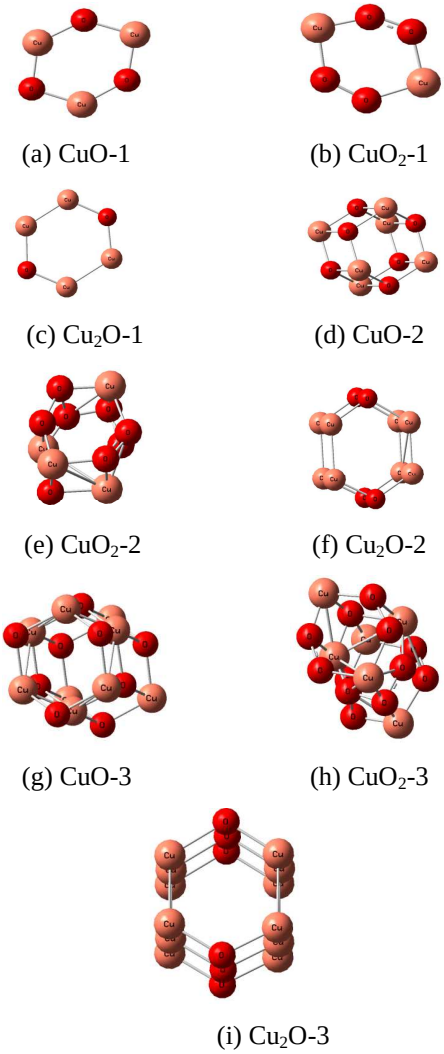

(a) CuO-1 (b) CuO_2-1

(c) Cu_2O-1 (d) CuO-2

(e) CuO_2-2 (f) Cu_2O-2

(g) CuO-3 (h) CuO_2-3

(i) Cu_2O-3

Fig 1. Optimized structures of CuO, CuO_2 and Cu_2O clusters

In the case CuO-2, CuO_2-2 and Cu_2O-2, they have two hexagonal layers one over the other with twelve atoms in total. In CuO-3, CuO_2-3 and Cu_2O-3 structures, the hexagonal layers are attached to the neighboring cluster forming a bee's hive like structures, considering all these types of realistic clusters, the energy, dipole moment and point symmetry are calculated and discussed.

Table 1 shows the calculated energy, dipole moment and point symmetry of CuO, CuO_2 and Cu_2O clusters. Among the structure of CuO-1, CuO_2-1 and Cu_2O-1 the energy for Cu_2O-1 is –6711.371 Hartrees which is more stable than the other structures, since in CuO_2-1 which is rich in oxygen atoms is least stable which has the energy of –3590.941 Hartrees. The dipole moment is maximum for CuO-1 due to asymmetry of the charge in the Cu and O atoms in the cluster which is found to be 2.335 Debye. Cu_2O-1 has the least dipole moment of 0.603 Debye, due to hexagonal structure in this type the point symmetry is C_s for all the three clusters. In the case of CuO-2, CuO_2-2 and Cu_2O-2 clusters also the same trend is noticed as like of the previous clusters, since two layers of hexagonal structures are formed one over the other layer.

Table 1. Energy, dipole moment (DM) and point symmetry of CuO, CuO_2 and Cu_2O clusters

Cluster	Energy (Hartrees)	DM (Debye)	Point symmetry
CuO-1	–5146.348	2.3356	C_S
CuO_2-1	–3580.941	0.8149	C_S
Cu_2O-1	–6711.371	0.6035	C_S
CuO-2	–10292.586	0.5059	C_1
CuO_2-2	–7159.896	3.1266	C_1
Cu_2O-2	–13420.906	0.5708	C_1
CuO-3	–12006.457	3.2664	C_S
CuO_2-3	–10440.506	0.0045	C_S
Cu_2O-3	–13569.948	0.0003	C_{2V}

In this type, Cu_2O cluster has the energy of –13420.90 Hartrees which is more stable than the other two structures. The dipole moment is maximum for CuO_2 structure which is 3.126 Debye and least for CuO-2 which is 0.505 Debye, for all the cluster the point symmetry is C_1. Interestingly, the energy increases for CuO-3, CuO_2-3 and Cu_2O-3 which has fourteen atoms in the cluster, Cu_2O-3 has the energy of –13567.948 Hartrees which is stable, CuO_2-3 has the energy of –10440.506 Hartrees which is least stable. The dipole moment is maximum for CuO-3 which is calculated to be 3.2664 Debye due to asymmetry in the structure. Both CuO_2-3 and Cu_2O-3 has low value of dipole moment which is 0.0045 and 0.0003 Debye respectively. The point symmetry for CuO-3 and CuO_2-3 is C_S and for Cu_2O-3 is C_{2V} which represents the asymmetry in the arrangement of atoms in the clusters. Comparing the energies of different clusters it is inferred that increase in the number of atoms in the cluster leads to the stability of the cluster.

3.2. HOMO-LUMO gap and density of states of CuO, CuO_2 and Cu_2O clusters

HOMO-LUMO gap of different clusters provides the insight for the electronic properties of clusters. Table 2 shows the energy gap between the HOMO-LUMO levels of different clusters. From the table it is seen that the gap of Cu_2O-1, Cu_2O-2 and Cu_2O-3 are 0.86, 1.21 and 0.59 eV respectively, this clearly indicate the metallic nature of the cluster than the other two type of clusters namely CuO and CuO_2.

Clearly it is also concluded that CuO_2-1, CuO_2-2 and CuO_2-3 have a gap of 1.64, 1.79 and 1.73 eV respectively, due to rich oxygen atoms in these clusters the energy gap is more which match well with the experimental results [25].

In a particular cluster, which is having high value of gap, requires more energy to lift the electrons from the HOMO level to LUMO level. In contrast, the cluster which has low value of gap requires less energy to move the electron from HOMO to LUMO level. From this it is seen in these clusters Cu_2O cluster have low gap which involves

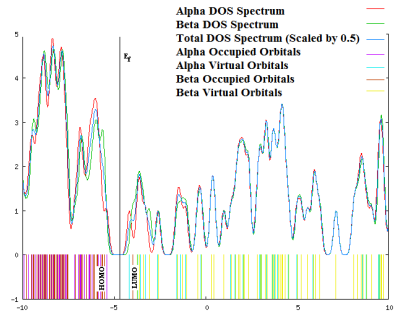

a CuO-1

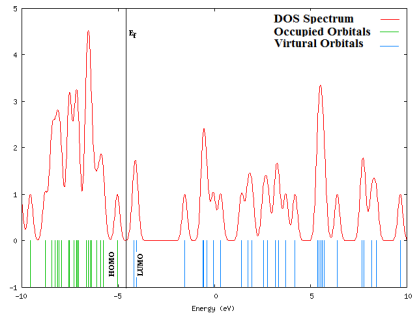

b CuO_2-1

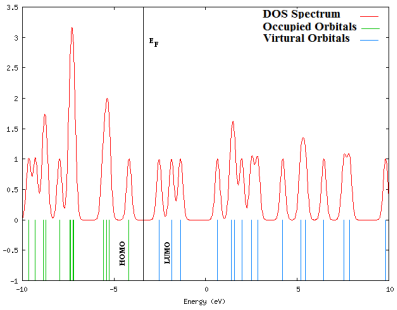

c Cu_2O-1

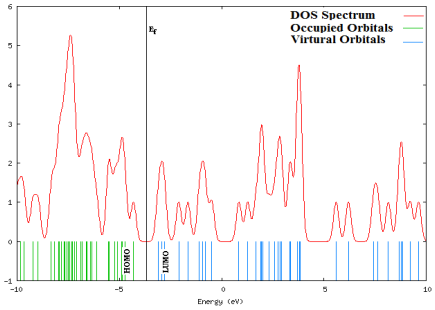

d CuO-2

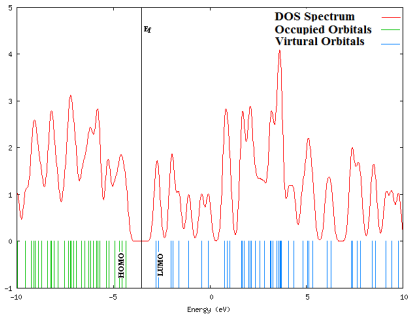

e CuO_2-2

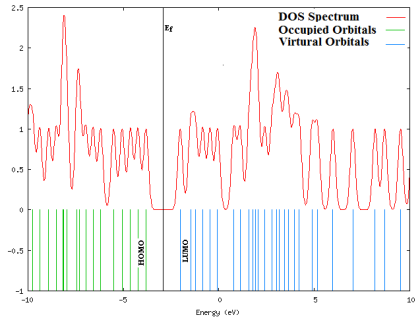

f Cu_2O-2

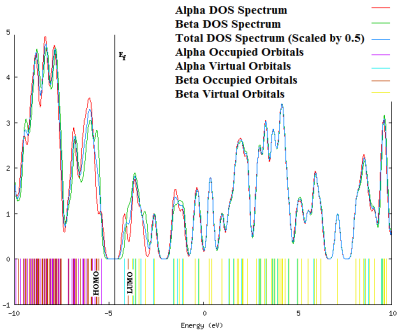

g CuO-3

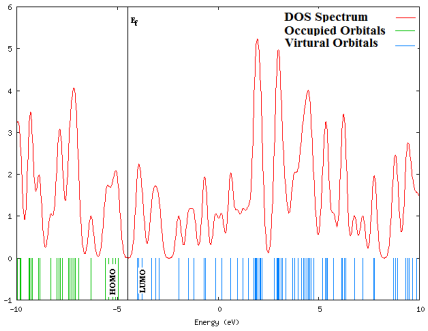

h CuO_2-3

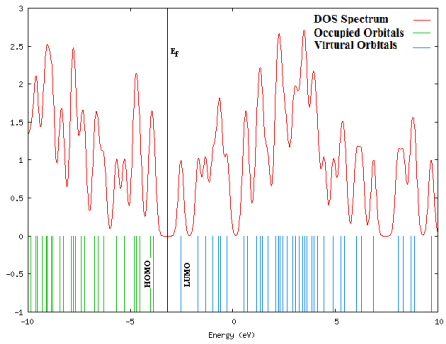

i Cu_2O-3

Fig. 2. DOS Spectrum and HOMO-LUMO gap of CuO, CuO_2 and Cu_2O clusters

low energy to move the electron from the clusters, CuO_2 requires more energy to lift the electron and CuO clusters have moderate energy gaps. Since lower energy gap materials are highly reactive in chemical reactions and with catalyst, Cu_2O-3 is highly reactive due to its lower energy gap. CuO-1 has the high value of band gap as 2.83 eV, which will not take part actively in chemical reactions.

Table 2. HOMO-LUMO gap of CuO, CuO_2 and Cu_2O clusters

Clusters	HOMO(eV)	LUMO(eV)	Eg(eV)
CuO-1	–5.83	–3.00	2.83
CuO_2-1	–4.18	–2.54	1.64
Cu_2O-1	–5.04	–4.18	0.86
CuO-2	–4.31	–3.10	1.21
CuO_2-2	–3.82	–2.03	1.79
Cu_2O-2	–4.31	–3.10	1.21
CuO-3	–4.82	–3.29	1.53
CuO_2-3	–3.85	–2.12	1.73
Cu_2O-3	–5.22	–4.63	0.59

The density of states (DOS) spectrum provides perception about the presence of the charge in the particular energy interval. In the case of CuO-1 due to the equal number of copper and oxygen atoms present in the cluster leads to the overlapping of orbitals. The electron with spin up will gives rise to alpha orbital and electrons with spin down will give rise to beta orbital. The alpha and beta orbital are seen only in the CuO-1 and CuO-3, whereas in the CuO-2 the presence of the atoms of copper and oxygen one over the other layer balance the spin of the electrons and no alpha and beta orbital are noticed in the case of CuO-2 cluster. Even in the DOS spectrum of CuO-1 the charges are far away from the Fermi level (E_F) which is noticed in the occupied orbitals. More number of peaks is observed in the virtual orbitals. In CuO_2 cluster the charges are localized near the Fermi level and wide gap is noticed between the adjacent levels in the virtual orbitals.

In CuO-2 cluster only some peak are seen in the occupied and virtual orbitals. In CuO_2-2 more broad density of charges are seen over wide energy range. Looking at the spectrum of Cu_2O-2 more number of periodic peaks is seen throughout the occupied and virtual orbitals again confirming more metallic nature. Analyzing the spectrum of CuO-3 the presence of more layers leads to broad peaks in occupied and virtual orbitals. In CuO_2-2 spectrum, maximum peak heights are noticed, which refer to the delocalization of charges in the virtual orbitals. Interesting observation in the case of Cu_2O-3 cluster is maximum peak heights are noticed throughout the occupied and virtual orbitals again confirms narrow band gap. The DOS provides the insight towards the density of the charges in the occupied and virtual orbitals. Figure 2, a – i, shows the DOS spectrum and HOMO-LUMO gap of CuO, CuO_2 and Cu_2O clusters respectively.

3.3. Ionization potential and electron affinity of CuO, CuO_2 and Cu_2O clusters

Fig. 3, Fig. 4 and Fig. 5 shows the ionization potential (IP) and electron affinities (EA) of CuO, CuO_2 and Cu_2O clusters. The ionization potential refers to the energy required to separate the electron from the cluster. Among all the clusters a high value of IP is noticed for CuO-1, Cu_2O-1 and Cu_2O-3 which has the IP of 5.83, 5.04 and 5.22 eV respectively this infers that these clusters will not actively take part in the chemical reactions. The high value of EA denotes the change in energy when an electron is added to the cluster, among all the clusters Cu_2O clusters found to have high value of EA due to more number of copper atoms in this clusters which shows slight metallic type of behaviour, Cu_2O clusters are more suitable for the chemical sensor applications since the change in energy takes place rapidly in these clusters [26, 27]. The EA of different nanoclusters are also in agreement with the reported results of Cu_nO_n for n = (1 – 8) clusters [28] and Cu_2O_x for x = (1 – 4) [29].

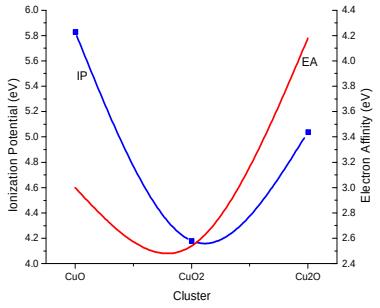

Fig. 3. Variation of ionization potential (IP) and electron affinity (EA) of CuO-1, CuO_2-1 and Cu_2O-1 clusters

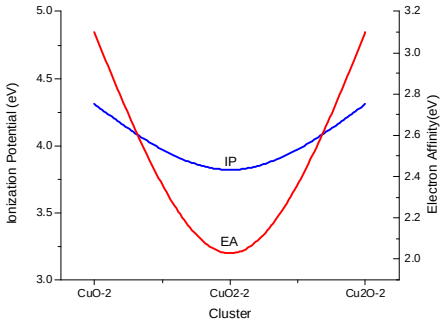

Fig. 4. Variation of ionization potential (IP) and electron affinity (EA) of CuO-2, CuO_2-2 and Cu_2O-2 clusters

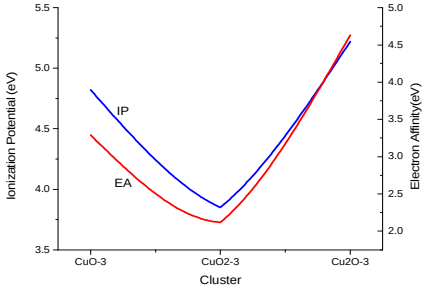

Fig. 5. Variation of ionization potential (IP) and electron affinity (EA) of CuO-3, CuO_2-3 and Cu_2O-3 clusters

3.4. Binding energies of CuO, CuO_2 and Cu_2O clusters

The binding energy (BE) per atom of CuO, CuO_2 and Cu_2O clusters for different structures are calculated using the following relation [30]:

$$BE = [(nE(Cu) + mE(O) - E(Cu_nO_m))/(n + m)], \quad (1)$$

where E(Cu) is the energy of Cu atom, E(O) is the energy of O atom, n and m are number of Cu and O atoms respectively. The calculated binding energies for different clusters are tabulated in Table 3. Among all the clusters CuO-1, CuO_2-1, Cu_2O-1 and CuO-2 has the BE of 4.38, 3.52, 3.50 and 4.13 eV respectively. The high value of BE infers that these clusters are stable; since all the clusters are having hexagonal structure, this results in high value of BE [31].

Table 3. Binding energies of CuO, CuO_2 and Cu_2O clusters

Clusters	BE (eV)
CuO-1	4.38
CuO_2-1	3.52
Cu_2O-1	3.50
CuO-2	4.13
CuO_2-2	1.95
Cu_2O-2	1.31
CuO-3	1.10
CuO_2-3	0.75
Cu_2O-3	2.25

4. CONCLUSION

The realistic nanoclusters of CuO, CuO_2 and Cu_2O are completely optimized using B3LYP/6-31G basis set. The energy, dipole moment and point symmetry of geometrically optimized nanoclusters are studied and discussed. The dipole moment arises due to the uneven charge distribution in the atoms of the different clusters. The stability of the clusters is discussed in terms of calculated energy, binding energy. The binding energies of CuO-1 and CuO_2-1, Cu_2O-1 and CuO-2 are found to be high among all the clusters. The high value of HOMO-LUMO gap is discussed which gives the information about the transition of electrons. DOS spectrum provides the perception about the presence of charge in various energy intervals. The high value of IP is noticed for CuO-1, Cu_2O-1 and Cu_2O-3 clusters. Cu_2O clusters have high value of EA which is due to the metallic nature of the cluster. The reported information will provide an insight for the experimentalist to synthesis new material which has its potential importance in the industrial applications.

REFERENCES

1. **Singh, N., Turner, A.** Leaching of Copper and Zinc from Spent Antifouling Paint Particles *Environmental Pollution* 157 2009: pp. 371 – 376.
2. **Guloyan, Yu. A.** Colloidal Coloring of Glasses: Unrecognized Nanotechnologies *Glass and Ceramics* 68 2011: pp. 171 – 181. http://dx.doi.org/10.1007/s10717-011-9347-3
3. **Malins, J. P., Tonge, K. H.** Reduction Processes in the Formation of Lustre Glazed Ceramics *Thermochimica Acta* 340 – 342 1999 : pp. 395 – 405.
4. **Oguchi, H., Kanai, H., Utani, K., Matsumura, Y., Imamura, S.** Cu_2O as Active Species in the Steam Reforming of Methanol by CuO/ZrO_2 Catalysts *Applied Catalysis A* 293 2005: pp. 64 – 70.
5. **Xiu, F. R., Zhang, F. S.** Preparation of nano-Cu_2O/TiO_2 Photocatalyst from Waste Printed Circuit Boards by Electrokinetic Process *Journal of Hazardous Materials* 172 2009: pp. 1458 – 1463.
6. **Hara, M., Hasei, H., Yashima, M., Ikeda, S., Takata, T., Kondo, J. N., Domen, K.** Mechano-catalytic Overall Water Splitting (II) Nafion-deposited Cu_2O *Applied Catalysis A* 190 2000: pp. 35 – 42.
7. **Tanaka, H., Shimakawa, T., Miyata, T., Sato, H., Minami, T.** Effect of AZO Film Deposition Conditions on the Photovoltaic Properties of AZO-Cu_2O Heterojunctions *Applied Surface Science* 244 2005: pp. 568 – 572. http://dx.doi.org/10.1016/j.apsusc.2004.10.121
8. **Chibber, S., Ansari, S. A., Satar, R.** New Vision to CuO, ZnO, and TiO_2 Nanoparticles: Their Outcome and Effects *Journal of Nanoparticle Research* 15 2013: pp. 1492. http://dx.doi.org/10.1007/s11051-013-1492-x
9. **Sato, M., Kameyama, T., Nonami, T.** Copper Polishing with a Polishing Pad Incorporating Abrasive Grains and a Chelating Resin *Precision Engineering* 33 2009: pp. 167 – 174.
10. **Yamauchi, H., Karppinen, M.** Hole-doping of the CuO_2 Planes in High Tc Superconductors *Materials Science and Engineering B* 54 1998: pp. 92 – 97.
11. **Mumtaz, M., Nawazish, A. Khan.** Reduced Anti-ferromagnetism Promoted by Zn $3d^{10}$ Substitution at CuO_2 Planar Sites of $Cu_{0.5}Tl_{0.5}Ba_2Ca_3Cu_4O_{12-\delta}$ Superconductors *Physica B* 404 2009 : pp. 3973 – 3977. http://dx.doi.org/10.1016/j.physb.2009.07.133
12. **Karppinen, M., Yamauchi, H., Morita, Y., Kitabatake, M., Motohashi, T., Liu, R. S., Lee, J. M., Chen, J. M.** Hole Concentration in the Three-CuO_2-Plane Copper-Oxide Superconductor Cu-1223 *Journal of Solid State Electrochemistry* 177 2004: pp. 1037 – 1043. http://dx.doi.org/10.1016/j.jssc.2003.10.011
13. **Ghosh, S., Avasthi, D. K., Shah, P., Ganesan, V., Gupta, A., Sarangi, D., Bhattacharya, R., Assmann, W.** Deposition of Thin Films of Different Oxides of Copper by RF Reactive Sputtering and their Characterization *Vacuum* 57 2000: pp. 377 – 385.
14. **Amikura, K., Kimura, T., Hamada, M., Yokoyama, N., Miyazaki, J., Yamada, Y.** Copper Oxide Particles Produced by Laser Ablation in Water *Applied Surface Science* 254 2008: pp. 6976 – 6982.
15. **Armelao, L., Barreca, D., Bertapelle, M., Bottaro, G., Sada, C., Tondello, E.** A Sol-Gel Approach to Nanophasic Copper Oxide Thin Films *Thin Solid Film* 442 2003: pp. 48 – 52.
16. **Casella, I. G., Gatta, M.** Anodic Electrodeposition of Copper Oxide:Hydroxide Films by Alkaline Solutions Containing Cuprous Cyanide Ions *Journal of Electroanalytical Chemistry* 494 2000: pp. 12 – 20.
17. **Endut, Z., Hamdi, M., Basirun, W. J.** Pseudocapacitive Performance of Vertical Copper Oxide Nanoflakes *Thin Solid Film* 528 2013: pp. 213 – 216.
18. **Dar, M. A., Kim, Y. S., Kim, W. B., Sohn, J. M., Shin, H. S.** Structural and Magnetic Properties of CuO Nanoneedles Synthesized by Hydrothermal Method *Applied Surface Science* 254 2008: pp. 7477 – 7481.
19. **Liu, L., Hong, K., Hu, T., Xu, M.** Synthesis of Aligned Copper Oxide Nanorod Arrays by a Seed Mediated Hydrothermal Method *Journal of Alloys and Compounds* 511 2012: pp. 195 – 197.

20. **Valiev, M., Bylaska, E. J., Govind, N., Kowalski, K., Straatsma, T. P., Van Dam, H. J. J., Wang, D., Nieplocha, J., Apra, E., Windus, T. L., deJong, W. A.** NWChem: A Comprehensive and Scalable Open-Source Solution for Large Scalemolecular Simulations *Computer Physics Communications* 181 2010: pp. 1477 – 1489.
21. **Bouklah, M., Harek, H., Touzani, R., Hammouti, B., Harek, Y.** DFT and Quantum Chemical Investigation of Molecular Properties of Substituted Pyrrolidinones *Arabian Journal of Chemistry* 5 2012: pp. 163 – 166.
22. **Mahfouz, R., Frag, E. A., Rafiq, M., Siddiqui, H., Al-kiali, W. Z., Karama, O.** New Aqua Rhenium Oxocomplex: Synthesis, Characterization, Thermal Studies, DFT Calculations and Catalytic Oxidations *Arabian Journal of Chemistry* 4 2011: pp. 119 – 124. http://dx.doi.org/10.1016/j.arabjc.2010.07.001
23. **Droghetti, A., Alfè, D., Sanvito, S.** Assessment of Density Functional Theory for Iron(II) Molecules Across the Spin-Crossover Transition *Journal of Chemical Physics* 137 2012: pp. 124303.
24. **Huang, W., Bulusu, S., Pal, R., Zeng, X. C., Wang, L. S.** CO Chemisorption on the Surfaces of the Golden Cages *Journal of Chemical Physics* 131 2009: pp. 234305.
25. **Chauhan, D., Satsangi, V. R., Dass, S., Shrivastav, R.** Preparation and Characterization of Nanostructured CuO Thin Films for Photoelectrochemical Splitting of Water *Bulletin of Materials Science* 29 2006: pp. 709 – 716.
26. **Zhan, C. G., Nichols, J. A., Dixon, D. A.** Ionization Potential, Electron Affinity, Electronegativity, Hardness, and Electron Excitation Energy: Molecular Properties from Density Functional Theory Orbital Energies *The Journal of Physical Chemistry A* 107 2003: pp. 4184 – 4195.
27. **Isseroff, L. Y., Carter, E. A.** Electronic Structure of Pure and Doped Cuprous Oxide with Copper Vacancies: Suppression of Trap States *Chemistry of Materials* 25 2013: pp. 253 – 265.
28. **Bae, G. T., Dellinger, B., Hall, R. W.** Density Functional Calculation of the Structure And Electronic Properties of CuO (n = 1 – 8) Clusters *Journal of Physical Chemistry A* 115 2011: pp. 2087 – 2095. http://dx.doi.org/10.1021/jp104177q
29. **Dai, B., Tian, L., Yang, J.** A Theoretical Study of Small Copper Oxide Clusters: Cu_2O_x x = 1 – 4 *Journal of Chemical Physics* 120 2004: pp. 2746 – 2751. http://dx.doi.org/10.1063/1.1638733
30. **Sriram, S., Chandiramouli, R.** A Study on the Electronic Properties of GaInPAs Nanostructures: A Density Functional Theory Approach *Europian Physical Journal Plus* 128 2013: pp. 116 1 – 8.
31. **Dwivedi, A., Misra, N.** Theoretical Study of Transition Metal Oxide Clusters (T_{MnOm}) [(TM– Pd, Rh, Ru) and (n, m = 1, 2)] *Journal of Atomic and Molecular Science* 297 2012: pp. 297 – 307 http://dx.doi.org/10.4208/jams.092511.102611a**.**